

# Transient Bragg fiber gratings formed by unpumped thulium doped fiber

Shui ZHAO<sup>1</sup>, Ping LU (✉)<sup>1,2</sup>, Li CHEN<sup>1</sup>, Deming LIU<sup>1,2</sup>, Jiangshan ZHANG<sup>3</sup>

<sup>1</sup> National Engineering Laboratory for Next Generation Internet Access System,  
Huazhong University of Science and Technology, Wuhan 430074, China

<sup>2</sup> School of Optical and Electronic Information, Huazhong University of Science and Technology, Wuhan 430074, China

<sup>3</sup> Department of Electronics and Information Engineering, Huazhong University of Science and Technology, Wuhan 430074, China

© Higher Education Press and Springer-Verlag Berlin Heidelberg 2013

**Abstract** A theoretical introduction of saturable absorber based on standing-wave saturation effects as a transient fiber Bragg grating (FBG) was presented. The central wavelength of the transient FBG was located in 2  $\mu\text{m}$ . The factors affecting the bandwidth and the reflectivity of the transient FBG were analyzed. The linewidth and reflectivity as the function of doped fiber length and doping concentration were correspondingly simulated by Matlab software. It was found that the larger the doping concentration and the fiber length were, the smaller the bandwidth was. These results suggest that the performance of the transient FBG can be optimized by choosing the appropriate length of doped fiber and the larger doping concentration, which can be used as a reference for the narrow-linewidth fiber laser around 2  $\mu\text{m}$ .

**Keywords** narrow-linewidth fiber laser, saturable absorber, thulium doped fiber (TDF)

## 1 Introduction

Since thulium doped fiber (TDF) lasers was proposed, it has been researched extensively in recent years for its attractive applications in atmospheric transmission, hydrocarbon gas sensing, laser lidar and eye safety [1,2]. The achievements of those researches on TDF lasers mainly concentrate on the topics, including high power, dispersion compensation,  $Q$ -switched and mode-locked [3–6]. However, few papers report narrow-linewidth and single longitudinal-mode fiber lasers around 2  $\mu\text{m}$  [7], and these lasers are very important in many applications involving

optical communications and optical fiber sensors [8]. As we all know, TDF can be used as a homogeneous broadening gain medium at room temperature, and its feature of strong mode competition results in mode hopping and unstable output [9]. A lot of methods have been used to attempt to obtain stable narrow-linewidth fiber lasers in C-band or L-band, such as using a fiber Bragg grating (FBG)-based Fabry-Perot (F-P) filter to increase longitudinal-mode spacing and achieve single frequency oscillation [10,11], adopting polarization incoherent technology [12] and constructing a ultrashort cavity for several centimeters as well as a high concentration gain fiber to realize the single frequency output [13].

One convenient way to achieve narrow-linewidth and single longitudinal-mode in fiber laser is using FBG as the filter, however the price of the FBG with linewidth around 2  $\mu\text{m}$  is too expensive, so the research about the transient Bragg fiber gratings formed by unpumped TDF is inevitable for its easy operation and excellent performance [14]. It has also been presented that the narrow-linewidth fiber laser can be obtained by inserting an unpumped doped fiber which acted as a saturable absorber for frequency selection and suppressing mode hopping [15]. Since Horowitz et al. presented this method in 1994 [16], more and more narrow-linewidth fiber laser using unpumped fiber as saturable absorber have been introduced, and they have achieved more excellent performance [17–19]. Although many works present configurations of narrow-linewidth fiber lasers using saturable absorber, they only focus on C-band or L-band [17,18]. So applying the mature theory of saturable absorber as the transient FBG to the new 2  $\mu\text{m}$  waveband can be useful and significant for the research of  $\text{Tm}^{3+}$  doped narrow linewidth fiber lasers, which have important applications such as gas sensors, wavelength-division multiplexing (WDM) optical communication technology and liquid water sensing [17]. In

this paper, we presented the theory of saturable absorber as a transient FBG based on standing-wave saturation effects, as well as analyzed the corresponding factors of parameters of a transient FBG.

## 2 Principle and methods

In fiber laser, there are usually two ways to realize the function of standing-wave saturation effects. One is the reflection structure including an unpumped doped fiber and a wavelength selection device such as a reflector or a FBG [18], the other is a Sagnac loop structure including a 3 dB coupler and an unpumped doped fiber, which can be used in both linear cavity and ring cavity [15]. The theoretical basis of operation have been shown in many works [19,20]. In the low doped fiber, two counter propagating waves meet and interference occur and form standing-wave saturation effects. The signal wave has strong absorption in the antinodes, and weak absorption in the nodal, resulting in periodical absorption coefficient change along the fiber axis. According to the Kramers-Kronig relation [21]:

$$\Delta n(z, \omega) = \frac{c}{\pi} P.V. \int_{\omega_1}^{\omega_2} \frac{\Delta \alpha(z, \omega')}{(\omega')^2 - \omega^2} d\omega', \quad (1)$$

where  $P.V.$  is the principal value of the integral derived and  $\omega_1 - \omega_2$  is the spectral range where the absorption is nonnegligible,  $\Delta \alpha(z, \omega')$  is the change in absorption,  $c$  is the speed of light. The variation of the absorption coefficient will result in periodical spatial variation of refraction index, which forms the transient Bragg reflection grating. For simplicity, the maximum change of refractive index that can be obtained in doped fiber can be described as [22]

$$\Delta n = \frac{\Gamma_s N \lambda \sigma_e}{4\pi}, \quad (2)$$

which is corresponding to that all of the particles in the ground state are excited to the upper state absorbing the energy of signal power. In the formula above,  $\Gamma_s$  is the filling factor accounting for the finite overlap between the signal mode and the concentration profile,  $N$  is the doping concentration of the unpumped fiber,  $\sigma_e$  is the emission cross-section of the doped particles. The period of the FBG is given by

$$\Lambda = \frac{\lambda_0}{2n_{\text{eff}}}, \quad (3)$$

which means the period varies with the change of resonant wavelength, and it acts as dynamic self-tracking narrow-linewidth filter. The established time of the FBG is decided by the excitation time of doped particles. The reflection of the FBG is written as [23]

$$R = \frac{\kappa^2 \sinh^2(\delta l)}{\delta^2 \cosh^2(\delta l) + \left(\frac{\Delta \beta}{2}\right)^2 \sinh^2(\delta l)}, \quad (4)$$

where  $\beta$  is the mode propagation constant,  $\kappa = \frac{\pi \gamma \Delta n}{\lambda}$  is the coupling coefficient of the FBG,  $\delta = \sqrt{\kappa^2 - \left(\frac{\Delta \beta}{2}\right)^2}$  is the detuning,  $l$  is the length of the doped fiber. The full width at half maximum (FWHM) of the FBG can be denoted as [24]

$$\Delta f = \frac{c}{\lambda} \kappa \sqrt{\left(\frac{\Delta n}{2n_{\text{eff}}}\right)^2 + \left(\frac{1}{N^*}\right)^2}, \quad (5)$$

where  $N^* = \frac{l}{\Lambda}$  is the number of grating periods,  $n_{\text{eff}} = 1.456$ .

In this paper, we choosed unpumped TDF as saturable absorber to simulate the reflection and FWHM of the transient FBG using Matlab software. If we treat the  $\text{Tm}^{3+}$  as a two-level system of  ${}^3\text{H}_6$  and  ${}^3\text{F}_4$ , the TDF will absorb the signal wave (1570 nm) and produce population inversion, forming a saturable absorber.

## 3 Simulation results

If we take the values:  $\Gamma_s = 0.752$ ,  $\sigma_e = 3 \times 10^{-25} \text{ m}^2$ ,  $N = 3.5 \times 10^{25} \text{ Tm}^{3+}/\text{cm}^3$ ,  $\lambda = 2000 \text{ nm}$  in Eq. (2), we can estimate  $\Delta n$  as  $1.257 \times 10^{-6}$ , and then we bring  $\Delta n$  into Eq. (4).

The property of TDF saturable absorber is related to the doping concentration of  $\text{Tm}^{3+}$  and the length of TDF. From Fig. 1, it can be observed that the simulative central Bragg wavelength is 2000 nm, and the saturable absorber has the biggest reflection in the central wavelength. We can also find in Fig. 1 that for stable change of refraction index  $\Delta n$ , the reflection of FBG became higher with the longer length of TDF (0.3, 0.5 and 0.7 m), while the FWHM became narrower. The relation between  $\Delta f$  and fiber length  $l$  is shown in Fig. 2,  $\Delta f$  decreases nonlinearly as  $l$  increases. We set  $l$  varying from 1 to 10 m, and we can get the linewidth of 14.45–130.4 MHz, or 0.1927–1.739 pm, which means the transient FBG can act as an ultra-narrow filter. Moreover, if the value of  $\Delta n$  decreases from  $1.257 \times 10^{-6}$  to  $3 \times 10^{-8}$  (see Fig. 3), the value of linewidth can be a few tenths of MHz and it can be seen as a single longitudinal-mode fiber laser if the linewidth is smaller than the free mode spacing. In theory, the FBG's filtering effect is more excellent with narrower  $\Delta f$  because less resonant modes are existed. If  $\Delta f$  is less than the longitudinal-mode spacing, one can achieve a single longitudinal-mode fiber laser. When it comes to the unpumped TDF, stable standing-wave saturation effects

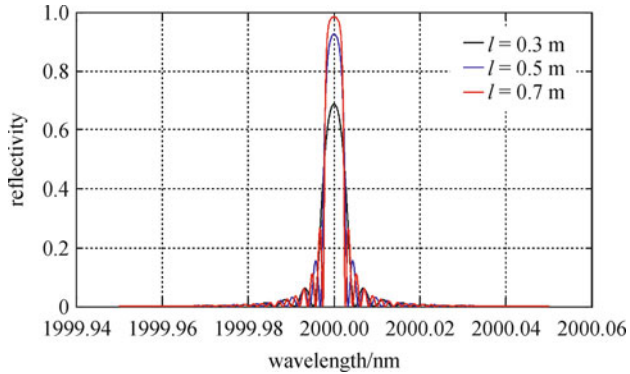


Fig. 1 Reflection spectrum of FBG with different fiber lengths

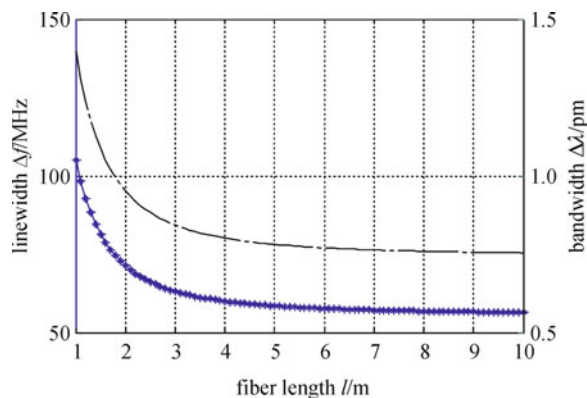


Fig. 2 Linewidth as a function of fiber length

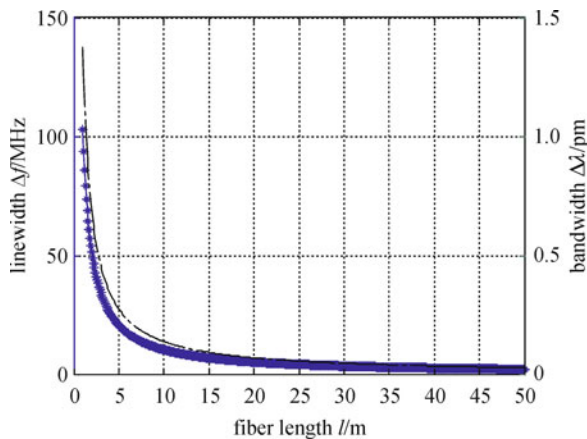


Fig. 3 Linewidth as a function of fiber length ( $\Delta n = 3 \times 10^{-8}$ )

cannot form with short length of doped fiber, so the longer length can achieve better performance. Even though, the threshold power will be higher, while the slope efficiency and the output power will get lower if we make the length of TDF too long because only the first half of it acts as a saturable absorber while the latter half become the attenuated fiber.

Another factor affecting the property of the transient

FBG is doping concentration,  $\Delta n$ . The reflection gets higher and FWHM gets broader with  $\Delta n$  increases from  $5 \times 10^{-7}$  to  $2 \times 10^{-6}$  (see Fig. 4), this result is consistent with the trend of Eqs. (4) and (5). Figure 5 shows the relation between reflection and fiber length with different  $\Delta n$ . Under the condition of higher  $\Delta n$ , the FBG reaches the highest reflection with shorter fiber length. Figure 6 shows the relationship between the linewidth of FBG and the doping concentration. The linewidth is inversely proportional to the doping concentration.

The power of the pump light is another inevitable factor for the performance of saturable absorber, the power of pump light cannot be too large. Generally, TDF can play the role of saturable absorber after depleting the pump light. The length of TDF depleting the pump light gets larger when the power of pump light gets bigger. Figure 7 shows the relationship between the length of saturable absorber (SA) and the power of pump light. That is to say, the remaining part of TDF acting as the saturable absorber is few under the larger pump power (setting the total length of TDF is fixed). So when the pump power is small, one can obtain the transient FBG with high reflectivity and narrow linewidth.

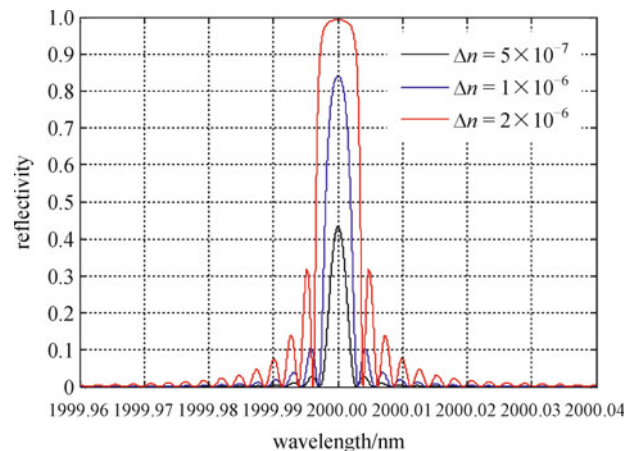


Fig. 4 Reflection spectrum of FBG with different  $\Delta n$

## 4 Discussion

The formation of TDF saturable absorber and its reflection as well as bandwidth are closely related to the doped fiber length and the doping concentration. In the experiment, we had better choose the length of TDF according to the laser intensity, pump power and the doping concentration, making it optimal to compress linewidth. However, when the TDF fiber length and the doping concentration are fixed, we can also achieve the optimal filtering effect and stable single longitudinal -mode by changing pumping power. Although other works have also presented the theory of the transient FBG, but they only focused on C-band or L-band [16,17]. This work may be used as reference for transient Bragg fiber

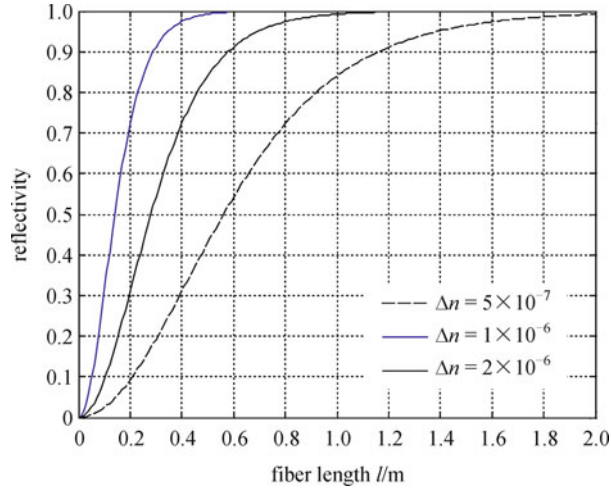


Fig. 5 Reflectivity of FBG as a function of fiber length with different  $\Delta n$

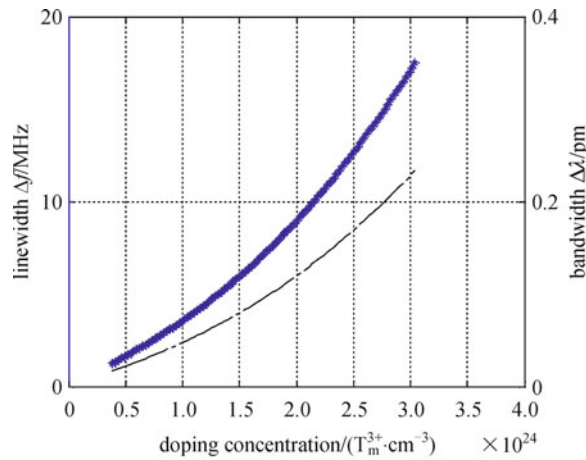


Fig. 6 Linewidth as a function of doping concentration  $N$

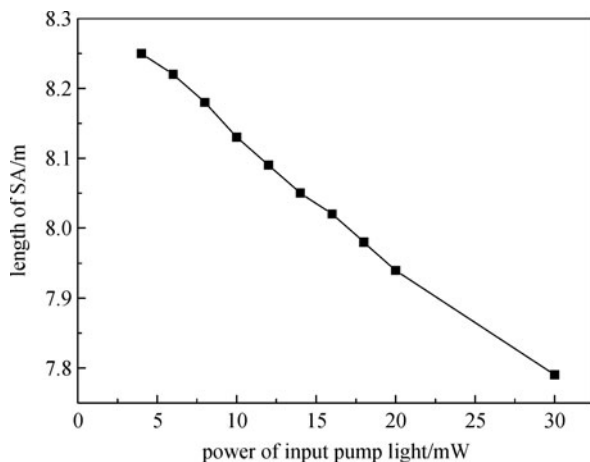


Fig. 7 Length of saturable absorber (SA) as a function of power of pump light

gratings formed by unpumped doped fiber near  $2 \mu m$ , which can be a useful and convenient way to obtain the narrow linewidth fiber laser.

## 5 Conclusions

In summary, we described the theory of the unpumped TDF acting as a saturable absorber. We used Matlab software to simulate the relation between reflectivity as well as FWHM of the transient FBG, and the doped fiber length as well as doping concentration. The reflectivity increases nonlinearly and  $\Delta f$  decreases correspondingly when fiber length increases. Meanwhile, the reflectivity increases nonlinearly and  $\Delta f$  increases correspondingly when doping concentration increases. In the experiment, we had better choose the length of TDF appropriately according to the laser intensity, pump power and the doping concentration, obtaining the perfect performance of narrow linewidth and single longitudinal-mode.

**Acknowledgements** This work was supported by the National Natural Science Foundation of China (Grant Nos. 61275083, 61290315).

## References

- Li D J, Du G G. The recent research progress of  $Tm^{3+}$ -doped fiber lasers. *Laser Technology*, 2007, 31(5): 540–543 (in Chinese)
- McAleavey F J, MacCraith B D, O’Gorman J, Hegarty J. Tunable and efficient diode-pumped  $Tm^{3+}$ -doped fluoride fiber laser for hydrocarbon gas sensing. *Fiber and Integrated Optics*, 1997, 16(4): 355–368
- Tang Y L, Xu L, Yang Y, Xu J Q. High-power gain-switched  $Tm^{3+}$ -doped fiber laser. *Optics Express*, 2010, 18(22): 22964–22972
- Wienke A, Haxsen F, Wandt D, Morgner U, Neumann J, Kracht D. Fiber based dispersion management in an ultrafast thulium-doped fiber laser and external compression with a normal dispersive fiber. In: *Proceedings of Advanced Solid-State Photonics*. San Diego: OSA Technical Digest, 2012, AT4A.26
- Geng J H, Wang Q, Smith J, Luo T, Amzajerdian F, Jiang S. All-fiber  $Q$ -switched single-frequency  $Tm$ -doped laser near  $2 \mu m$ . *Optics Letters*, 2009, 34(23): 3713–3715
- Wang Q, Geng J, Luo T, Jiang S. Mode-locked  $2 \mu m$  laser with highly thulium-doped silicate fiber. *Optics Letters*, 2009, 34(23): 3616–3618
- Geng J H, Wang Q, Luo T, Jiang S B, Amzajerdian F. Single-frequency narrow-linewidth  $Tm$ -doped fiber laser using silicate glass fiber. *Optics Letters*, 2009, 34(22): 3493–3495
- Shen Y H, Zhao W Z, He J L, Sun T, Grattan K T V. Fluorescence decay characteristic of  $Tm$ -doped YAG crystal fiber for sensor applications, investigated from room temperature to  $1400^\circ C$ . *IEEE Sensors Journal*, 2003, 3(4): 507–512
- Moulton P F, Rines G A, Slobodtchikov E V, Wall K F, Frith G, Samson B, Carter A L G.  $Tm$ -doped fiber lasers: fundamentals and power scaling. *IEEE Journal on Selected Topics in Quantum*

- Electronics, 2009, 15(1): 85–92
10. He X, Fang X, Liao C, Wang D N, Sun J. A tunable and switchable single-longitudinal-mode dual-wavelength fiber laser with a simple linear cavity. *Optics Express*, 2009, 17(24): 21773–21781
  11. Sun J Q, Yuan X H, Zhang X L, Huang D X. Single-longitudinal-mode fiber ring laser using fiber grating-based Fabry-Perot filters and variable saturable absorbers. *Optics Communications*, 2006, 267(1): 177–181
  12. Chang D I, Guy M J, Chernikov S V, Taylor J R, Kong H J. Single-frequency erbium fibre laser using the twisted-mode technology. *Electronics Letters*, 1996, 32(19): 1786–1787
  13. Kaneda Y, Spiegelberg C, Geng J H, Hu Y D, Luo T, Wang J F, Jiang S B. 200-mw, narrow-linewidth 1064.2-nm Yb-doped fiber laser. In: *Proceedings of Lasers and Electro-Optics, CLEO. 2004, 2: Cth03:1–2*
  14. Yang J, Qu R G, Sun G Y, Geng J X, Cai H W, Fang Z J. Suppression of mode competition in fiber lasers by using a saturable absorber and a fiber ring. *Chinese Optics Letters*, 2006, 4(7): 410–412
  15. Frisken S J. Transient Bragg reflection gratings in erbium-doped fiber amplifiers. *Optics Letters*, 1992, 17(24): 1776–1778
  16. Horowitz M, Daisy R, Fischer B, Zyskind J L. Linewidth-narrowing mechanism in lasers by nonlinear wave mixing. *Optics Letters*, 1994, 19(18): 1406–1408
  17. Yin F F, Yang S G, Chen H W, Chen M H, Xie S Z. Tunable single-longitudinal-mode Ytterbium all fiber laser with saturable-absorber-based auto-tracking filter. *Optics Communications*, 2012, 285(10–11): 2702–2706
  18. He X Y, Wang D N. Tunable and switchable dual-wavelength single-longitudinal-mode Erbium-doped fiber lasers. *Journal of Lightwave Technology*, 2011, 29(6): 842–849
  19. Kishi N, Yazaki T. Frequency control of a single-frequency fiber laser by cooperatively induced spatial-hole burning. *IEEE Photonics Technology Letters*, 1999, 11(2): 182–184
  20. Horowitz M, Daisy R, Fischer B, Zyskind J L. Linewidth-narrowing mechanism in lasers by nonlinear wave mixing. *Optics Letters*, 1994, 19(18): 1406–1408
  21. Fleming S, Whitley T. Measurement and analysis of pump dependent refractive index and dispersion effects in erbium-doped fiber amplifiers. *IEEE Journal of Quantum Electronics*, 1996, 32(7): 1113–1121
  22. Desurvire E. Study of the complex atomic susceptibility of Erbium-doped fiber amplifiers. *Journal of Lightwave Technology*, 1990, 8(10): 1517–1527
  23. Kashyap R. *Fiber Bragg Gratings*. SanDiego: Academic press, 1999
  24. Othonos A, Kalli K. *Fiber Bragg Gratings: Fundamentals and Applications in Telecommunications and Sensing*. Norwood, MA: Artech House, 1999